ELSEVIER

Journal of Power Sources 68 (1997) 208–211

JOURNAL OF POWER SOURCES

# X-ray photoelectron spectroscopy analyses of lithium intercalation and alloying reactions on graphite electrodes

H. Momose [a,*], H. Honbo [a], S. Takeuchi [a], K. Nishimura [a], T. Horiba [b], Y. Muranaka [a], Y. Kozono [a], H. Miyadera [a]

[a] *Hitachi Research Laboratory, Hitachi, Ltd., 7-1-1, Omika-cho, Hitachi, Ibaraki 319-12, Japan*

[b] *Saitama Research Laboratory, Shin-Kobe Electric Machinery Co., Ltd., Okabe-machi, Ohsato-gun, Saitama 369-02, Japan*

Accepted 31 October 1996

**Abstract**

Electrochemical lithium intercalation reactions occurring in silver-supported graphite anodes were investigated by X-ray photoelectron spectroscopy (XPS). The binding energy of Li(1s) of intercalating lithium was higher than that of lithium metal, which suggests that lithium exists in the form of a positive ion in the graphite layers. The core level of the C(1s) signal of lithium intercalated graphite was higher than that of graphite, which implies that the carbon in lithium-intercalated graphite has a negative charge. This finding agrees with previous XPS studies indicating that carbon has a negative charge in a graphite-intercalation compound produced by a molten lithium intercalation reaction to graphite. Lithium carbonate, lithium fluoride and organic compounds were produced on the graphite surfaces in charge/discharge reactions in 1 M $LiPF_6$/EC–DMC electrolytic solution. It was also confirmed that the initial charge current supplied to the graphite electrode with a potential between 2.8 and 0.6 V did not cause a lithium-intercalation reaction. It caused, however, other reactions such as decomposition of the electrolytic solution and production of passivating films. © 1997 Published by Elsevier Science S.A.

*Keywords:* Lithium batteries; X-ray photoelectron spectroscopy; Graphite; Anodes

## 1. Introduction

Various materials have been investigated as the anode materials for a lithium-ion secondary battery having a high energy density and long cycle life. For example, new metal–graphite composite anodes in the form of ultrafine silver particles supported on a graphite surface were developed to provide a higher volumetric specific capacity and longer cycle life than conventional graphite anodes [1]. In this paper, the chemical states of new metal–graphite composite anodes are studied using X-ray photoelectron spectroscopy (XPS). XPS has been used for analyses of graphite intercalation compounds (GICs) produced by a molten lithium intercalation reaction with graphite [2,3]. It was also used for analyses of the surface film on a carbon black anode in lithium secondary cells [4].

In the present study, electrochemical lithium intercalation and alloying reactions occurring in silver-supported graphite electrodes were investigated. An irreversible reaction, which caused low coulombic efficiency in the first charge/discharge cycle, was also examined.

## 2. Experimental

Metal–graphite composite electrodes were prepared as follows. Ultrafine silver particles were deposited on graphite from an aqueous solution of $Ag^+$ using hydrazine as a reducing agent. The silver–graphite (Ag–G) powder was dispersed into a mixture of diethylbenzene and ethylene–propylene terpolymer and was coated on a copper foil which acted as a current collector. The binder percentage in the anode was 10 wt.%. The loading of the Ag–G was about 5 mg/cm$^2$. The 1.0 M $LiPF_6$/ethylene carbonate (EC)–dimethyl carbonate (DMC) system was used as an electrolytic solution. Electrochemical measurements were carried out in an argon-filled glove box to avoid oxidation of the lithium–Ag–G composite. Charging was done in a three-electrode cell, lithium foils were used as the reference and counter electrodes. After the charge/discharge process, the sample electrodes were removed from the electrochemical cell and rinsed with dimethoxyethane (DME) in order to remove the electrolyte. After rinsing, the sample electrodes were dried in an argon glove box at room temperature until the DME evaporated. The sample electrodes were kept in a transfer vessel filled with argon gas, and then were transferred to the XPS apparatus.

* Corresponding author.


*PII* S0378-7753(96)02627-4

All the XPS measurements were performed using a Shimadzu/Kratos AXIS-HSi instrument. The monochromatized X-ray source (Al K$\alpha$) was used. Energy resolution was about 0.71 eV. The binding energy was calibrated using Au($4f_{7/2}$) at 84.0 eV. The macro-mode (about 0.4 mm × 0.6 mm) was selected as the measurement area condition to get information on the Ag–G electrodes. Argon-ion etching was used to get concentration depth profiles which provided elemental and chemical information. The etching rate was estimated as 5 A/min for silica.

## 3. Results and discussion

Fig. 1 shows the X-ray diffraction (XRD) pattern of 10wt.%Ag–graphite (Ag–G) composite powder. Peaks of both silver metal and graphite were confirmed, implying that silver was deposited not as an oxide, but as a metal. Scanning electron microscopy and energy dispersive X-ray (SEM–EDX) images of the Ag–G powder indicated that silver particles were disseminated on the graphite surface.

Fig. 2 shows the change in the potential versus $Li^+/Li$ of the Ag–G electrode during the first charge. The charge current density was kept constant at 0.5 mA/cm$^2$. The charge finally stopped when the potential of the Ag–G electrode reached 0.0 V versus $Li^+/Li$. To investigate the chemical states of the Ag–G electrode in the middle of the first charge, XPS measurements were made for electrodes charged to 0.6 and 0.1 V.

Fig. 3 shows the XRD pattern of an Ag–G electrode which was charged to 0.01 V versus $Li^+/Li$. The surfaces of the charged electrodes turned to golden yellow. Signals of $LiC_6$ and $LiC_{12}$ were detected, indicating the formation of GICs

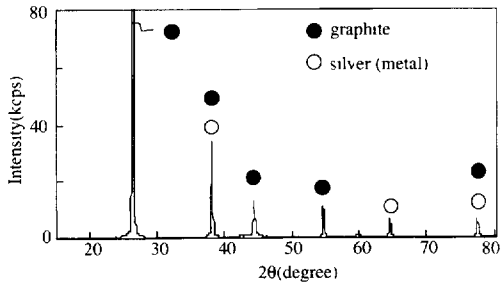


Fig. 1. XRD pattern of 10wt.%Ag–graphite powder.

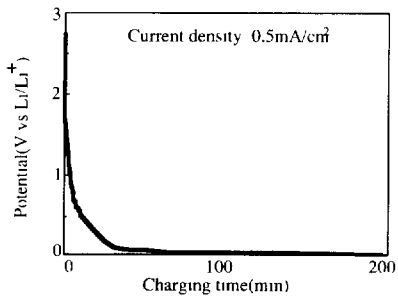


Fig. 2. Potential change of an Ag–graphite composite electrode during the first charging.

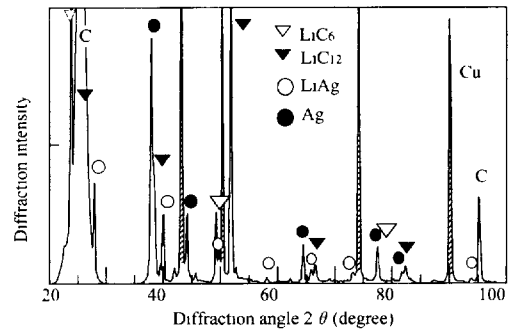


Fig. 3. XRD pattern of charged 10wt.%Ag–graphite electrode

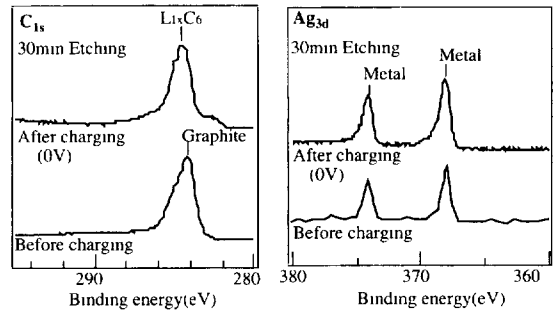


Fig. 4. XPS spectra of Ag–graphite electrodes.

during the charge. The signals of LiAg showed that the silver particles alloyed with doped lithium. This suggested that Ag–G anodes use both an intercalation reaction and an alloying reaction. The Cu signals in the diffraction pattern were due to the copper foil which acted as a current collector.

In the XPS measurements of charged Ag–G electrodes, signals of C, Ag, O, F and P were detected. Fig. 4 shows the Li(1s) spectra of the Ag–G electrodes charged to 0 V. The binding energy of the main peak of Li(1s) of the doped lithium was higher than that of lithium metal. This suggested that most of the lithium exists in the form of positive ions in the graphite layers. The atomic concentration of silver in 10wt.%Ag–graphite is less than 2%, so intercalating lithium in graphite forms a major part of the lithium doping in the Ag–G electrodes. A peak regarded as lithium fluoride or lithium carbonate was contained in the Li(1s) spectrum of an electrode etched for 2 min, suggesting that a reaction other than lithium intercalation or an alloying reaction occurs on the electrode.

Fig. 5 shows C(1s) and Ag(3d) XPS spectra of the Ag–G electrodes, the upper curves are spectra of a charged electrode and the lower ones are spectra of an uncharged electrode. The binding energy of C(1s) of lithium-intercalated graphite was higher than that of graphite by 0.5 eV. Previous XPS studies on GIC produced by reactions between molten lithium and highly orientated pyrolytic graphite (HOPG) [2,3] indicate that the Fermi level of carbon in a GIC shifts due to charge redistribution and the core level of C(1s) in a GIC is higher than that of graphite. The C(1s) spectrum of charged graphite in Fig. 5 was also considered to be influenced by the Fermi level shift which was estimated to be $1.3 \pm 0.2$ eV. The core level of C(1s) of lithium-intercalated

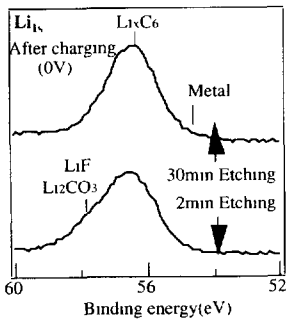


Fig. 5. XPS spectra of Ag–graphite electrodes.

graphite was higher than that of conventional graphite by 0.8 eV, which suggested that the carbon in the lithium-intercalated graphite may have a negative charge. The binding energy of Ag(3d) indicated a metallic state after charging. Fig. 6 shows a diagram of the energy states which were determined in this study. Fig. 7 shows the XPS spectra of F(1s) and O(1s) of the charged Ag–G electrodes. These signals indicate the formation of lithium fluoride, lithium carbonate, lithium oxide and organic compounds on the graphite surfaces during the charge process.

Fig. 8 shows the depth profiles of the amount of lithium in the Ag–G electrodes during the first charge. The amounts of lithium were estimated from the signal intensity ratio of Li(1s)/C(1s). It was confirmed that the first charge current supplied to an electrode with a potential between 2.8 and 0.6 V did not cause either lithium-intercalation or alloying reactions. Instead, reactions such as decomposition of the electrolytic solution and formation of passivating films occurred. Fig. 9 shows the C(1s) spectrum of an Ag–G electrode which was charged to the potential of 0.1 V. The appearance of the peak for lithium carbonate suggest the decomposition of electrolytic solvents and an irreversible reaction on the electrode during charging

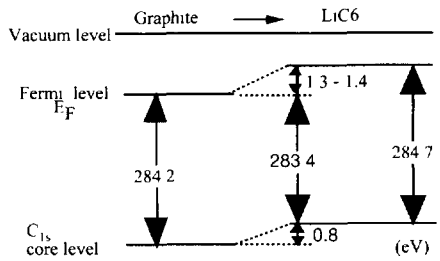


Fig. 6. Energy states of Ag–graphite electrodes obtained from XPS spectra.

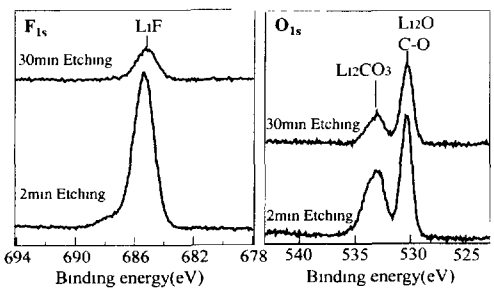


Fig. 7. XPS spectra of Ag–graphite electrodes.

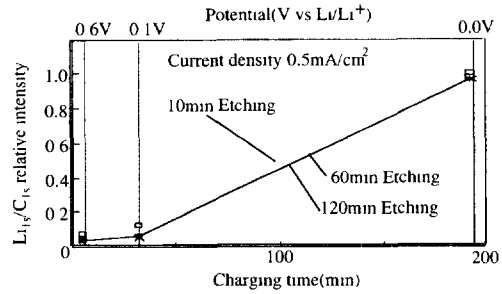


Fig. 8. Profiles of lithium in an electrode during the first charging.

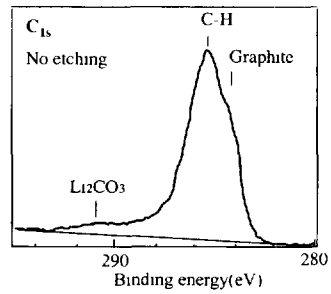


Fig. 9. C(1s) XPS spectrum of an electrode charged to the potential of 0.1 V.

$$EC + 2Li^+ + 2e^- \rightarrow Li_2CO_3 + C_2H_4$$

$$LiPF_6 + H_2O \rightarrow LiF + 2HF + POF_3 \text{ (in the solvent)}$$

$$2Li^+ + 2HF + 2e^- \rightarrow 2LiF + H_2$$

$$Li_2CO_3 + 2HF \rightarrow 2LiF + H_2CO_3$$

The decomposition of $LiPF_6$ by $H_2O$ is known [5]. $H_2O$ was contained in the electrolytic solution and the electrode as an impurity. The decomposition of EC and the formation of lithium carbonate have been suggested in a study on the reductive reaction of alkyl carbonate solutions on the graphite electrode surface [6].

Fig. 10 shows the depth profiles of C, O, Li, Ag, F in the Ag–G electrodes charged to 0.1 and to 0.0 V. The relative

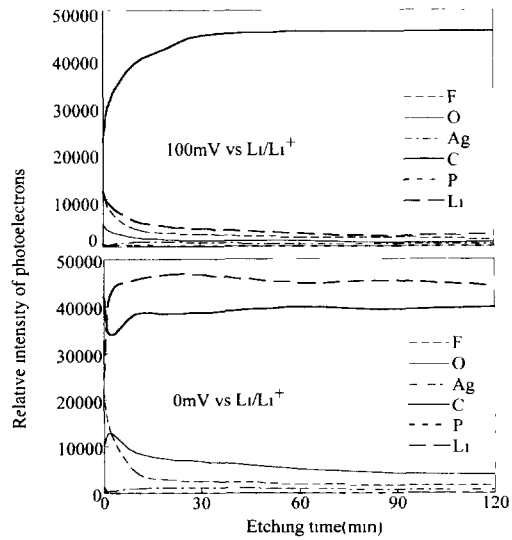


Fig 10. Depth profiles of elements in an electrode during the first charging.

intensity of photoelectrons was calculated by dividing the counts of each element by the sensitivity factor of each element. Because the relative intensity of P is nearly zero, the profile of P was omitted in Fig. 10. The depth profile of the Ag–G electrode charged to 0.1 V indicated that a decline in lithium concentration occurred inside the electrode. In the profile of the Ag–G electrode charged to 0.0 V, the relative intensity of lithium was very large compared with the intensity of carbon, when lithium and carbon are present in $LiC_6$. This result indicated that the sensitivity factor used for lithium was actually greater and the sensitivity factor for carbon was actually smaller. Both profiles of electrodes charged to 0.1 and to 0.0 V, respectively, indicated that oxygen and fluorine were concentrated within the surface of the electrode. This indicated probably a passivation film being formed by lithium fluoride and lithium carbonate.

## 4. Conclusions

XRD spectra showed that the Ag–G anode used not only an intercalation reaction, but also an alloy reaction for the battery reaction. The XPS spectra showed that intercalating lithium was in an ionic state and the graphite carbon was in a negatively charged state. The surface of the graphite anode was covered by lithium fluoride and lithium carbonate. In the first charge process, another reaction between the electrode surface and the electrolytic solution, occurred and a passivation film was formed on the electrode surface. One of the reasons for the low coulombic efficiency in the first charge/discharge cycle was this irreversible reaction.

## Acknowledgements

This work was financially supported by New Energy and Industrial Technology Development Organization (NEDO).

## References

[1] K. Nishimura et al., *Ext. Abstr., 8th Int. Meet. Lithium Batteries, Nagoya, Japan, 1996*, pp. 338–339.
[2] G.K. Wertheim, P.M Th.M. Van Attekum and S. Basu, *Solid State Commun., 33* (1980) 1127–1130.
[3] U.M. Gubler, V. Geiser, P. Oelhafen, H.J. Guntherodt, J Evers and A Weiss, *Synth. Met., 8* (1983) 141–145
[4] K. Takei, K. Kazuma, Y. Kobayashi, H. Miyashiro, T. Iwahori, T. Uwai and H. Ue, *J. Power Sources, 54* (1995) 171–174
[5] D.W.A. Sharp, *Adv Fluorine Chem., 1* (1960) 69.
[6] H. Yoshida et al., *Proc. 36th Battery Symp Japan, Kyoto, Japan, 1995*, pp. 101–102.